Solar cell with an intermediate band of finite width

Michael Y. Levy*
Insituto de Energía Solar, Universidad Politécnica de Madrid, 28040 Madrid, Spain

Christiana Honsberg†
Department of Electrical and Computer Engineering, University of Delaware, Newark, Delaware 19716, USA
(Received 7 July 2008; published 27 October 2008)

This article considers idealized solar cells whose absorbers are intermediate band (IB) media with finite bandwidths that permit both interband and intraband photoinduced electronic transitions at states within the IB. To comprehend the effect of the IB width, three classes of IB absorbers are constructed where each class is distinguished from the others by its spectral selectivity. It is shown that (i) the maximum-power efficiency tends gradually toward zero with increasing bandwidth when photoinduced interband transitions and intraband transitions are equally likely; (ii) with respect to the former, a relative efficiency enhancement may occur when photoinduced intraband transitions dominate interband transitions; and (iii) although thermodynamically consistent, efficiencies may be physically inconsistent without including photoinduced intraband transitions. Resulting from the solar surface temperature of 6000 K, the authors conclude that the largest efficiencies result when the IB width is roughly equal to or less than 800 meV.

DOI: 10.1103/PhysRevB.78.165122 PACS number(s): 84.60.Jt, 71.55.−i, 85.60.−q, 89.30.Cc

I. INTRODUCTION

In 1960, Wolf[1] explained that the performance of a solar cell with multiple photoinduced electronic transitions may surpass that of a single-junction solar cell. Multiple transitions are allowed because of electronic states located at energies intermediate to those of the conduction and valence bands. In 1997, Luque and Martí[2] established that the upper efficiency limit of a solar cell with electronic states that form a single intermediate band (IB) with infinitesimal bandwidth is 63.2%. Although an idealized intermediate band solar cell (IBSC) is formed with an IB of infinitesimal bandwidth,[2] a finite bandwidth may be linked to the concentration of atoms that provide the electronic states intermediate to those of the conduction and valence bands.[3] Many candidate material systems are proposed to realize absorbers appropriate for these solar cells.[4–13] The candidate material systems are characterized by intermediate bands whose widths are of the order of 100 meV[5,11–13] or even 1 eV.[4,6–10] In an earlier work,[14] the authors examined IB width and showed that although thermodynamically consistent,[15] the results of detailed-balance calculations may be physically inconsistent when photoinduced intraband transitions are excluded or ignored.[14]

The present paper quantifies the impact of both finite IB width and spectral selectivity on the optimized detailed-balance conversion efficiencies of the IBSC and its associated band structure. The work is significant as it shows that (i) finite bandwidths result in a graceful degradation in the efficiency and (ii) the most suitable band structures for solar energy conversion differ significantly depending on the IB width and on the spectral selectivity of the absorbing medium. Beyond its use in identifying materials for an IBSC, resulting from its emphasis on an absorber that permits both intraband and interband transitions at intermediate levels, the paper provides a more comprehensive understanding of a general class of optoelectronic devices with intermediate states, i.e., up[16] and down converters[17] and multiband solar cells.[18]

As shown in Fig. 1, the absorber of this cell contains quantum states forming an IB of width $\Delta\varepsilon_{\mathrm{IB}}$. Resulting from the states of the IB, there are three allowed photoinduced interband electronic transitions[2] between a state in the IB and one in the valence band (I,V), between a state in the conduction band and one in the IB (C,I), and between a state in the conduction band and one in the valence band (C,V). In addition there are photoinduced intraband electronic transitions between two distinct states in the IB, (I,I). Thus, the set of allowed photoinduced electronic transitions of an IBSC absorber, $\mathcal{T}$, is defined as $\mathcal{T}\doteq\{(\mathrm{I},\mathrm{I}),(\mathrm{I},\mathrm{V}),(\mathrm{C},\mathrm{I}),(\mathrm{C},\mathrm{V})\}$.[14] Resulting from the three interband transitions, the IBSC is thermodynamically equivalent[14] to a tandem stack of three single-junction, single-transition solar cells electrically assembled by a series/parallel connection[19] (the latter tandem stack is such that a solar cell with a large band gap is electrically connected in parallel to two solar cells with smaller band gaps that are electrically connected to each other in series) so that its efficiency limit (63.2%)[2] has an upper ceil-

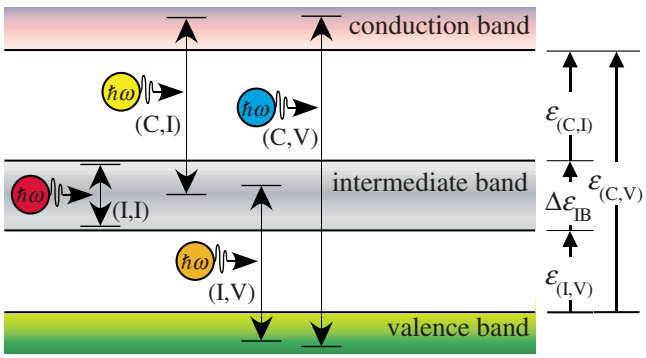

FIG. 1. (Color online) Reduced band structure of an intermediate band solar cell absorber. The band gaps between bands X and Y, $\varepsilon_{(X,Y)}$, are shown as well as the intermediate band's width, $\Delta\varepsilon_{\mathrm{IB}}$. Also illustrated is the set, $\mathcal{T}$, of photoinduced electronic transitions: {(I,I), (I,V), (C,I), and (C,V)}.

ing at the limit of a tandem stack of three unconstrained single-junction, single-transition solar cells (63.8%).[20]

The efficiency of an IBSC is obtained by calculating six photon flows:[2,14] one photon flow absorbed by and one photon flow emitted from the converter resulting from each of the three interband electronic transitions. To describe each photon flow resulting from (X,Y) transitions, the absorption coefficients are relevant twice. First, the sum of the absorption coefficients, $\Sigma_{i\in\mathcal{T}}\alpha_i$, appears in the absorptivity, a, as[21]

$$a(\hbar\omega)=\frac{[1-R(\hbar\omega)]\left[1-\exp\left(-d\sum_{i\in\mathcal{T}}\alpha_i\right)\right]}{1-R(\hbar\omega)\exp\left(-d\sum_{i\in\mathcal{T}}\alpha_i\right)}, \quad (1)$$

where i is an index into the set $\mathcal{T}$, $\hbar$ is Planck's constant, and ω is the radian frequency of the photons. The above absorptivity is derived from expressions for the overall transmission[22] and overall reflection[22] of radiant power in an intermediate band absorbing medium that permits multiple internal reflections,[22] which has a thickness d and a surface reflectivity R. Second, the absorption coefficient $\alpha_{(X,Y)}$ appears normalized in terms of the sum as[14]

$$\frac{\alpha_{(X,Y)}(\hbar\omega)}{\sum_{i\in\mathcal{T}}\alpha_i(\hbar\omega)}.$$

The remainder of the paper is organized as follows. In Sec. II the authors logically construct the three distinct IB absorbers where each is distinguished by its spectral selectivity and then give an explicative example that plainly describes the mathematical functions that yield the idealized spectral selectivity. Next, in Sec. III the authors discuss the maximum-power solar energy conversion efficiencies of an IBSC implemented with each of these three absorbers and the electronic band structures associated with these efficiencies. Next, in Sec. IV the authors offer concluding remarks.

II. SPECTRAL SELECTIVITY

This section is divided into two parts. In Sec. II A the authors present a logical description of the idealized spectral selectivity of IB absorbers. The resulting spectral selectivity is given mathematically in terms of Heaviside functions. Next in Sec. II B the authors offer an explicative example that visually reinforces the nature of the idealized spectral selectivity.

A. Formalism

Here, the authors construct three classes of IB absorbers, each distinguished by its normalized absorption coefficients. To do this, attention is first directed to a band structure where the band gaps $\varepsilon_{(X,Y)}$ (see Fig. 1) are spread within the domain of large solar irradiance. Next, even though the detrimental impact of absorption overlap on the performance of the solar cell is explained in Ref. 23, the advantage of its inclusion is demonstrated here. Finally, the interplay between spectral selectivity and intraband transitions is considered.

TABLE I. This table gives the onsets, $\alpha^{\mathrm{on}}_{(X,Y)}$, and offsets, $\alpha^{\mathrm{off}}_{(X,Y)}$, of photon exchange due to (X,Y) transitions that lead to optimum maximum-power efficiencies. They are given for the three classes of intermediate band solar cell absorbers such that when there is the possibility of both photoinduced interband and intraband electronic transitions, each of the transitions are equally likely, they are limited to interband electronic transitions, or they are limited to intraband electronic transitions.

	Equally likely	Limited to interband	Limited to intraband
$\alpha^{\mathrm{on}}_{(\mathrm{I,I})}$	0	0	0
$\alpha^{\mathrm{off}}_{(\mathrm{I,I})}$	$\Delta\varepsilon_{\mathrm{IB}}$	$\min(\varepsilon_{(\mathrm{I,V})},\Delta\varepsilon_{\mathrm{IB}})$	$\Delta\varepsilon_{\mathrm{IB}}$
$\alpha^{\mathrm{on}}_{(\mathrm{I,V})}$	$\varepsilon_{(\mathrm{I,V})}$	$\varepsilon_{(\mathrm{I,V})}$	$\max(\varepsilon_{(\mathrm{I,V})},\Delta\varepsilon_{\mathrm{IB}})$
$\alpha^{\mathrm{off}}_{(\mathrm{I,V})}$	$\varepsilon_{(\mathrm{C,I})}+\varepsilon_{\mathrm{vp}}$	$\varepsilon_{(\mathrm{C,I})}+\varepsilon_{\mathrm{vp}}$	$\max(\varepsilon_{(\mathrm{C,I})}+\varepsilon_{\mathrm{vp}},\Delta\varepsilon_{\mathrm{IB}})$
$\alpha^{\mathrm{on}}_{(\mathrm{C,I})}$	$\varepsilon_{(\mathrm{C,I})}$	$\varepsilon_{(\mathrm{C,I})}$	$\max(\varepsilon_{(\mathrm{C,I})},\Delta\varepsilon_{\mathrm{IB}})$
$\alpha^{\mathrm{off}}_{(\mathrm{C,I})}$	$\varepsilon_{(\mathrm{C,V})}$	$\varepsilon_{(\mathrm{C,V})}$	$\max(\varepsilon_{(\mathrm{C,V})},\Delta\varepsilon_{\mathrm{IB}})$
$\alpha^{\mathrm{on}}_{(\mathrm{C,V})}$	$\varepsilon_{(\mathrm{C,V})}$	$\varepsilon_{(\mathrm{C,V})}$	$\max(\varepsilon_{(\mathrm{C,V})},\Delta\varepsilon_{\mathrm{IB}})$
$\alpha^{\mathrm{off}}_{(\mathrm{C,V})}$	$\lim\rightarrow\infty$	$\lim\rightarrow\infty$	$\lim\rightarrow\infty$

When $\varepsilon_{(\mathrm{I,V})}$, $\varepsilon_{(\mathrm{C,I})}$, and $\varepsilon_{(\mathrm{C,V})}$ are spread within the domain of high solar irradiance, it is ideal if photons join two electronic states separated by the largest band gap less than the photons' energies. This is because photon interaction with matter is associated with a rate of internal irreversible entropy generation, which increases monotonically with $(\hbar\omega-\mu_{(X,Y)})$,[24] where $\mu_{(X,Y)}$ is the potential difference of the carriers in bands X and Y. The normalized absorption coefficients yield this spectral selectivity if (i) the occupancy of the electronic states located at energies intermediate to those of the conduction and valence bands is such that the densities of filled and empty states are of the same order of magnitude[1] (in other words, the intermediate band absorber is metallic[25]); (ii) beginning at the onset of (C,I) transitions, the product of the matrix elements of momentum and joint density of states[26] governing (C,I) transitions is orders larger than that governing (I,V) transitions, and (iii) beginning at the onset of (C,V) transitions, the (C,V) product is orders greater than the (C,I) product.

The ideal spectral selectivity must accommodate an overlap, $\varepsilon_{\mathrm{vp}}$, between photoabsorption due to (I,V) transitions and photoabsorption due to (C,I) transition. Allow that for the band structure leading to the limiting efficiency [i.e., $\varepsilon_{(\mathrm{I,V})}=0.71$ eV, $\varepsilon_{(\mathrm{C,I})}=1.24$ eV, and $\varepsilon_{(\mathrm{C,V})}=1.95$ eV (Ref. 2)] the maximum-power point (MPP) of the IBSC is such that each of the constituent engines[14] are at their respective MPP. All else equal, save that the upper IB edge increases so that $\varepsilon_{(\mathrm{C,I})}$ goes from 1.24 to 0.71 eV, the following ensues from the spectral selectivity above. The net photon flow that is absorbed due to (I,V) transitions, goes to zero, and because of the current constraint of the IBSC,[2,14] the operating point of the (C,I) engine goes from its MPP to its open-circuit point. The ideal spectral selectivity must accommodate that for photons within a range $(\varepsilon_{(\mathrm{C,I})}\leq\hbar\omega\leq\varepsilon_{(\mathrm{C,I})}+\varepsilon_{\mathrm{vp}}<\varepsilon_{(\mathrm{C,V})})$, the absorption coefficients $\alpha_{(\mathrm{C,I})}$ and $\alpha_{(\mathrm{I,V})}$ overlap as $\alpha_{(\mathrm{C,I})}(\hbar\omega)=\alpha_{(\mathrm{I,V})}(\hbar\omega)$. In this way, the (I,V) and (C,I) engines may be simultaneously biased at their MPP.

With regard to the allowed intraband transitions, the authors consider IB absorbers classified in one of three ways.

For the situation where $\Delta\varepsilon_{\mathrm{IB}}$ is larger than the smallest band gap in the system, the absorbers may be distinguished by the absorption properties for photons within the range ($\Delta\varepsilon_{\mathrm{IB}} \leq \hbar\omega < \min \varepsilon_{(X,Y)}$). The first class of absorbers is distinguished so that photoinduced intraband electronic transitions and photoinduced interband electronic transitions are equally likely. For this class, for photons in the specified range, all of the nonzero absorption coefficients are of equal value. The second class of absorbers is distinguished so that photon exchange within this range is solely coupled to intraband transitions. Thus, in this range, the absorption coefficients $\alpha_{(\mathrm{I,V})}$, $\alpha_{(\mathrm{C,I})}$, and $\alpha_{(\mathrm{C,V})}$ are null. The third is distinguished so that photoinduced electronic transitions are solely coupled to interband transitions so that the absorption coefficient $\alpha_{(\mathrm{I,I})}$ is null within this range.

The authors, therefore, write the ideal normalized absorption coefficients as

$$\frac{\alpha_{(X,Y)}(\hbar\omega)}{\sum_{i\in\mathcal{T}} \alpha_i(\hbar\omega)} = \frac{H(\hbar\omega - \alpha^{\mathrm{on}}_{(X,Y)}) - H(\hbar\omega - \alpha^{\mathrm{off}}_{(X,Y)})}{\sum_{i\in\mathcal{T}} [H(\hbar\omega - \alpha^{\mathrm{on}}_{i}) - H(\hbar\omega - \alpha^{\mathrm{off}}_{i})]}, \quad (2)$$

where the Heaviside step functions, H, indicate the ideal absorption onsets and offsets for each of the three classes of IB absorbers. [Note that $H(x)$ is defined so that it equals to 0 or to 1 if x is less than or greater than zero, respectively.[27]] The onset and offset of photon exchange due to (X,Y) transitions begin with photons with energies greater than or equal to $\alpha^{\mathrm{on}}_{(X,Y)}$ and $\alpha^{\mathrm{off}}_{(X,Y)}$, respectively. Table I gives these values for each class of IB absorbers, where it is uniformly assumed that $\varepsilon_{(\mathrm{C,I})} \geq \varepsilon_{(\mathrm{I,V})}$. In obtaining these results, a simplifying assumption is made: for any range of photon energies, all nonzero absorption coefficients within this range are of equal value. Thus, the normalized absorption coefficients may take the following values: 0, 1/3, 1/2, or 1. In the next section, detailed-balance results are presented and explained.

B. Explicative example

In this subsection the authors offer an explicative example to reinforce the formal description of the idealized normalized absorption coefficients. In panel (a) of Fig. 2, the authors plot the emission spectrum, $\dot{n}$, of a black body with a surface temperature of 6000 K. This spectrum approximates the emission spectrum of the Sun and sets the order of magnitude of each of the band gaps, $\varepsilon_{(X,Y)}$, that are useful for solar energy conversion. Please note that Wien's energy, $\hbar\omega_W$—the abscissa value at which the emission spectrum peaks—of a black body with a temperature of 6000 K is 825 meV. As solar energy science is fundamentally linked to the Plank spectrum of a black body and as the Plank spectrum is a statistical distribution, the abscissa value of the statistical mode is useful as a point of reference. Wien's energy will be used by the authors to frame the discussion of detailed-balance results and in the conclusions of this paper.

In panels (b)-(e) of Fig. 2, the authors plot the idealized normalized absorption coefficients for a hypothetical absorbing medium. The absorbing medium has a band structure, whereby $\Delta\varepsilon_{\mathrm{IB}}$, $\varepsilon_{(\mathrm{I,V})}$, $\varepsilon_{(\mathrm{C,I})}$, and $\varepsilon_{(\mathrm{C,V})}$ are equal to 300, 600, 1200, and 2100 meV, respectively, and has an absorption overlap, $\varepsilon_{\mathrm{vp}}$, within a 300 meV range. According to Eq. (2) and to any of the three columns of Table I, the onsets of photon exchange (i.e., $\alpha^{\mathrm{on}}_{(X,Y)}$) resulting from (I,I), (I,V), (C,I), and (C,V) are equal to 300, 600, 1200, and 2100 meV, respectively. Further, the offsets of photon exchange (i.e., $\alpha^{\mathrm{off}}_{(X,Y)}$) resulting from (I,I), (I,V), and (C,I) are equal to 300, 1500, and 2100 meV, respectively. Resulting from the absorption overlap of the hypothetical absorber considered here, photons with the energies in the range $1200 \leq \hbar\omega \leq 1500$ meV experience two parallel-absorption paths,[28] meaning that photons with energies in the aforementioned range may be absorbed by inducing either an (I,V) electronic transition or a (C,I) electronic transition. Further, based on the idealizations constructed herein, which are made explicit by Eq. (2), an incident photon within the aforementioned range induces an (I,V) transition with one-half probability and a (C,I) transition with one-half probability. In the following section, the authors present and discuss the results of detailed-balance calculations, where these calculations are made with spectral selectivity defined herein.

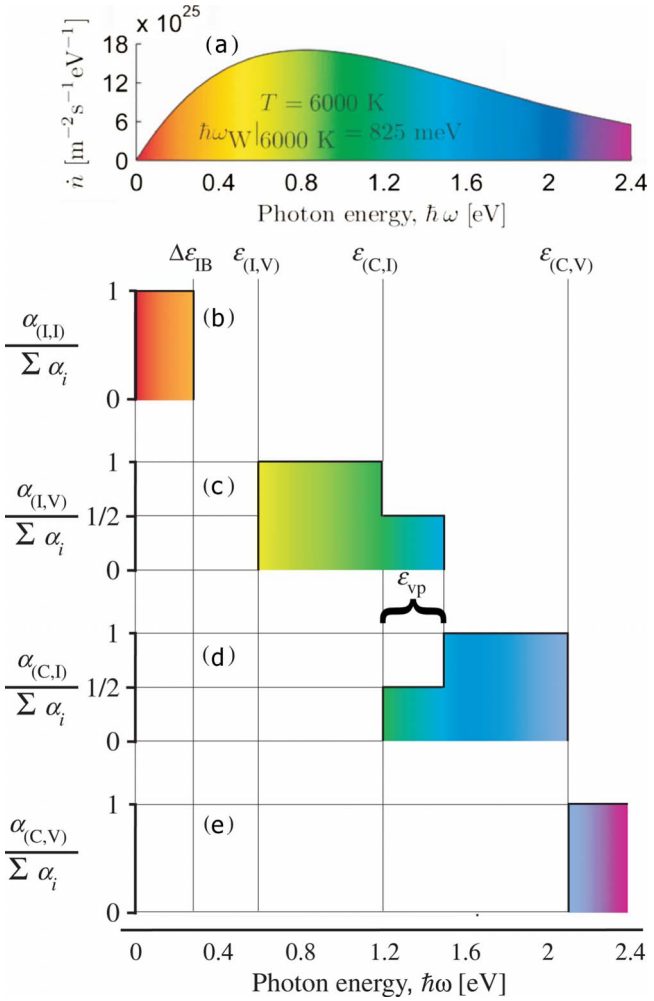

FIG. 2. (Color online) (a) Emission spectrum of a black body that approximates that of the sun. Wien's energy, $\hbar\omega_W$, is labeled. (b)-(e) idealized normalized absorption coefficients of a hypothetical intermediate band absorber.

III. RESULTS AND DISCUSSION

In this section, the authors present the optimized efficiencies of IBSC (Fig. 3). This is done for each of the three classes of IB absorbers. In addition, the authors present the band gaps (Fig. 4) and the absorption overlaps (Fig. 5) associated with these efficiencies. The results for each of the three classes of IB absorbers are compared and contrasted. As explained in Sec. II B, Wien's energy is employed as an energetic reference while discussing the results.

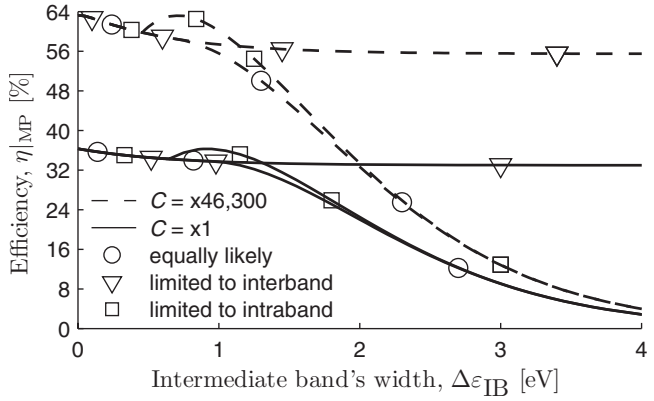

FIG. 3. Maximum-power efficiency of intermediate band solar cell as a function of the intermediate band's width. Curves are given for two geometrical concentration factors and for three classes (see Table I) of intermediate band absorbers. The concentrations are the maximum physically realizable concentration (×46 300) and nonconcentrated (×1) solar illuminations. Limiting efficiency of 63.2% occurs when $\Delta\varepsilon_{IB}$ is 15 meV.

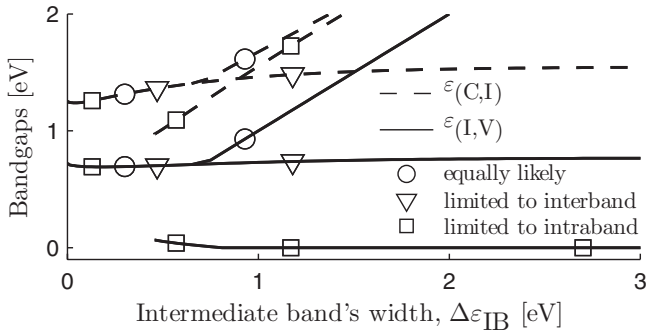

FIG. 4. Band gaps $\varepsilon_{(I,V)}$ and $\varepsilon_{(C,I)}$ associated with efficiencies given in Fig. 3. Results given for a concentration of ×46 300.

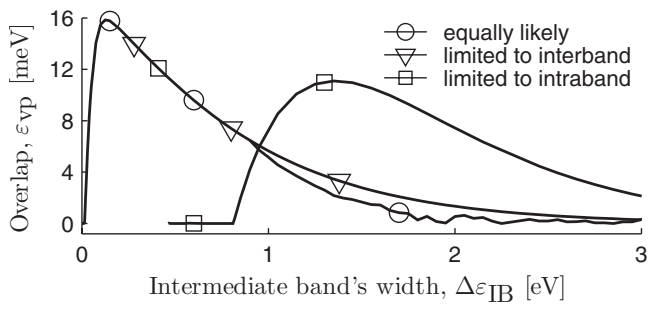

FIG. 5. Overlap (see Fig. 2 and Table I) between (I,V) and (C,I) absorptions. Results associated with efficiencies of Fig. 3 for a concentration of ×46 300.

Figure 3 presents the efficiencies[36] of the solar cell calculated at maximum power, $\eta|_{MP}$, as a function of intermediate band width. In calculating the results, the detailed-balance formalism of Ref. 14 is used with the Sun and Earth given as black bodies with surface temperatures of 6000 and 300 K, respectively, and a converter whose temperature is that of the Earth's surface. Further, nonradiative recombination is null, multiple electron-hole generation is nonexistent, and photoabsorptance is unity for all photons that join electronic transitions (i.e., the absorber's thickness is semi-infinite and the absorber's surface reflectivity is null). For each value of $\Delta\varepsilon_{IB}$, $\eta|_{MP}$ is found with an optimization routine that treats $\varepsilon_{(I,V)}$, $\varepsilon_{(C,I)}$, and ε_{vp} as parameters in the search space. In precisely computing the photon flows, the method in Ref. 29 is used. Results are given for the three classes of IB absorbers and two values of geometric concentration, the maximum physically realizable concentration of isotropic solar irradiance in air/vacuum[30–32] (×46 300) and nonconcentrated (×1) solar illumination.

With respect to the class of IB absorbers such that photoinduced interband transitions and intraband transitions are equally likely whenever there is the physical possibility of both, Fig. 3 shows that $\eta|_{MP}$ monotonically decreases to zero with respect to $\Delta\varepsilon_{IB}$. Although not visible, the data indicates that for the case of the maximum concentration there is a short lived increase in efficiency so that the limiting IBSC efficiency (63.19%) is achieved for a bandwidth of 15 meV. Brown *et al.*[33] noted this perceptible increase. Figure 4 gives the band gaps $\varepsilon_{(I,V)}$ and $\varepsilon_{(C,I)}$ associated with $\eta|_{MP}$. When $\Delta\varepsilon_{IB}$ is less than or equal to 800 meV, which is of the order of Wien energy of a black body at 6000 K, $\hbar\omega_W|_{6000\ K}$, the optimum values of $\varepsilon_{(I,V)}$ is no more than 100 meV less than $\hbar\omega_W|_{6000\ K}$. Further, $\varepsilon_{(C,I)}$ is roughly 400–500 meV greater than $\hbar\omega_W|_{6000\ K}$. When $\Delta\varepsilon_{IB}$ is greater than $\hbar\omega_W|_{6000\ K}$, the optimum values of $\varepsilon_{(I,V)}$ maintains the value of $\Delta\varepsilon_{IB}$ so as to minimize losses due to nonwork producing intraband transitions. Figure 5 gives the absorption overlaps, ε_{vp}, associated with $\eta|_{MP}$. The associated absorption overlaps are less than 20 meV.

With respect to the class of IB absorbers such that photon exchange is limited to interband electronic transitions whenever there is the physical possibility of both interband and intraband transitions, the data indicate that as $\Delta\varepsilon_{IB}$ increases, $\eta|_{MP}$, $\varepsilon_{(I,V)}$, and $\varepsilon_{(C,I)}$ saturate. On saturating, the efficiency and their associated band gaps are those of an optimized series-connected two-stack tandem solar cell.[34] These indicate that as $\Delta\varepsilon_{IB}$ increases, the power absorbed due to (C,V) electronic excitations steadily decreases. Ultimately, the photoinduced (C,V) excitations offer negligible contribution as there are relatively few photons in the solar spectrum with such high energies. That the IBSC operates as a two-junction solar cell results from the stringent condition that photoinduced electronic transitions are limited to interband transitions and the solar cells current and voltage constraints.[2,14]

Although the detailed-balance method is thermodynamically consistent,[15] the results obtained for this class are not physically consistent for large bandwidths. As $\Delta\varepsilon_{IB}$ increases toward infinity, the electronic band structure appears as that of a black body. Although a black body may produce a heat flux, no photovoltaic work may be produced because all the

carriers are in thermodynamic equilibrium. The more $\Delta\varepsilon_{IB}$ exceeds $\hbar\omega_W|_{6000\ K}$, the more physically inconsistent are the results.

With regards to the class of IB absorbers with photon exchange limited to intraband electronic transitions whenever there is the physical possibility of both interband and intraband transitions, Fig. 3 shows that the trajectories of the efficiencies follow similar courses as those of the class where absorption is equally likely up until $\Delta\varepsilon_{IB}$ equals 0.46 and 0.65 eV, respectively, for concentrations of $\times 46\,300$ and $\times 1$. At these bandwidths this class offers a relative efficiency enhancement with respect to class where absorption is equally likely.

A solar cell with this class of absorbers exploits the fact that the absorption onset due to (I,V) transitions is limited by $\Delta\varepsilon_{IB}$ rather than by $\varepsilon_{(I,V)}$. The upshot is that the internally biased chemical-potential difference, $\mu_{(I,V)}$, is no longer limited from above by $\varepsilon_{(I,V)}$ but rather by $\Delta\varepsilon_{IB}$. Additionally, $\varepsilon_{(I,V)}$ is no longer relevant in calculating the net photon flux absorbed due to (I,V) transitions; so it may be decreased if it enhances the performance of the solar cell. Figure 4 shows that a performance gain is indeed obtained by a concomitant reduction in $\varepsilon_{(C,I)}$ and $\varepsilon_{(C,V)}$ so that the onsets of optical absorption are spaced more evenly across the range of high solar irradiance; consequently, there is an increase in the net photon flux absorbed due to both (C,I) and (C,V) transitions. In theory, the value of $\varepsilon_{(I,V)}$ may not approach arbitrarily close to zero because at some threshold[35] the rate of nonradiative interband transitions induced by phonon emission may no longer be ignored. In such a case, the premises of the equilibrium analysis[24] are violated for the carriers in the valence band and IB would be brought to thermodynamic equilibrium by the phonon exchanges. In the following section, the authors offer concluding remarks based on the detailed-balance results.

IV. CONCLUSIONS

This article quantifies the effect of the intermediate band's width, $\Delta\varepsilon_{IB}$, and spectral selectivity on the performance of intermediate band solar cells. Irrespective of the geometric concentration factor and resulting from the solar surface temperature, the authors conclude that the largest efficiencies result when $\Delta\varepsilon_{IB}$ is roughly equal to or less than 825 meV: Wien's energy of a black body with a surface temperature of 6000 K. For example, when $\Delta\varepsilon_{IB}$ equals 825 meV, the first-law efficiencies reach 57.9% and 33.9% (compared with 63.2% and 36.3% when $\Delta\varepsilon_{IB}=0$) for fully concentrated and nonconcentrated solar illumination, respectively. Thus, when $\Delta\varepsilon_{IB}$ is less than or roughly equal to 825 meV, the solar cell efficiency retains over 90% of its optimum value. When $\Delta\varepsilon_{IB}$ is less than or roughly equal to 825 meV, in order to achieve high efficiencies at large concentrations, the smallest and next smallest band gap ought to be roughly 100 meV smaller and 400–500 meV larger than 825 meV, respectively. Finally, when $\Delta\varepsilon_{IB}$ is greater than the smallest band gap, photoinduced intraband transitions need to be included for physical consistency.

ACKNOWLEDGMENTS

This work was supported by the U.S. National Renewable Energy Laboratory through Subcontract No. XAT-5-44277-01, which is administered by M. Symko-Davies and R. McConnell. This work was partially supported by the U.S. National Science Foundation International Research Fellowship Award No. OISE-0701460, which is administered by S. Parris.

*mail2MYL@gmail.com; qb@ies-def.upm.es
†honsberg@UDel.ece.edu

[1] M. Wolf, Proceedings of the Institute of Radio Engineers, 1960 (unpublished), Vol. 48, pp. 1246–1263.
[2] A. Luque and A. Martí, Phys. Rev. Lett. **78**, 5014 (1997).
[3] E. F. Schubert, in *Doping in III-V Semiconductors*, edited by H. Ahmed, M. Pepper, and A. Broers (Cambridge University Press, Cambridge, UK, 1993), Chap. 1, pp. 41–44.
[4] P. Wahnón and C. Tablero, Phys. Rev. B **65**, 165115 (2002).
[5] K. M. Yu, W. Walukiewicz, J. Wu, W. Shan, J. W. Beeman, M. A. Scarpulla, O. D. Dubon, and P. Becla, Phys. Rev. Lett. **91**, 246403 (2003).
[6] C. Tablero, A. J. García, J. J. Fernández, P. Palacios, and P. Wahnón, Comput. Mater. Sci. **27**, 58 (2003).
[7] C. Tablero and P. Wahnón, Appl. Phys. Lett. **82**, 151 (2003).
[8] J. Fernández, C. Tablero, and P. Wahnon, J. Chem. Phys. **120**, 10780 (2004).
[9] C. Tablero, P. Palacios, J. Fernández, and P. Wahnón, Sol. Energy Mater. Sol. Cells **87**, 323 (2005).
[10] P. Palacios, J. J. Fernández, K. Sanchez, J. C. Conesa, and P. Wahnon, Phys. Rev. B **73**, 085206 (2006).
[11] C. Tablero, Phys. Rev. B **74**, 195203 (2006).
[12] C. Tablero, Sol. Energy Mater. Sol. Cells **90**, 203 (2006).
[13] C. Tablero, J. Chem. Phys. **123**, 114709 (2005).
[14] M. Y. Levy and C. Honsberg, J. Appl. Phys. (to be published).
[15] A. Luque, A. Martí, and L. Cuadra, IEEE Trans. Electron Devices **48**, 2118 (2001).
[16] P. Gibart, F. Auzel, J.-C. Guillaume, and K. Zahraman, Jpn. J. Appl. Phys., Part 1 **35**, 4401 (1996).
[17] T. Trupke, M. A. Green, and P. Würfel, J. Appl. Phys. **92**, 1668 (2002).
[18] A. S. Brown and M. A. Green, J. Appl. Phys. **94**, 6150 (2003).
[19] T. Trupke and P. Würfel, J. Appl. Phys. **96**, 2347 (2004).
[20] A. Martí and G. L. Araújo, Sol. Energy Mater. Sol. Cells **43**, 203 (1996).
[21] M. Y. Levy and C. Honsberg, Proceedings of the Fourth WCPEC (IEEE 06CH37747), Waikoloa, HI, 2006 (unpublished), pp. 71–74.
[22] J. I. Pankove, in *Optical Processes in Semiconductors*, Prentice-Hall Electrical Engineering Series and Solid State Physical Electronics Series Vol. 11 (Prentice-Hall, Englewood Cliffs, NJ, 1971), pp. 93–94.
[23] L. Cuadra, A. Martí, and A. Luque, IEEE Trans. Electron Devices **51**, 1002 (2004).

[24] P. Würfel, J. Phys. C **15**, 3967 (1982).
[25] A. Luque and A. Martí, Prog. Photovoltaics **9**, 73 (2001).
[26] P. Bardeen, F. Blatt, and L. H. Hall, Photoconductivity Conference, Atlantic City, NJ, 1954 (unpublished), p. 147.
[27] *Standard Mathematical Tables and Formulae*, 30th ed., edited by D. Zwillinger (CRC, Boca Raton, FL, 1996).
[28] M. Y. Levy, N. J. Ekins-Daukes, and C. Honsberg, Proceedings of the EUPVSEC 22, Milan, Italy, 2007 (unpublished), pp. 432–435.
[29] M. Y. Levy and C. Honsberg, Solid-State Electron. **50**, 1400 (2006).
[30] W. Shockley and H. J. Queisser, J. Appl. Phys. **32**, 510 (1961).
[31] A. DeVos, *Endoreversible Thermodynamics of Solar Energy Conversion* (Oxford University Press, Oxford, 1992), pp. 76–77.
[32] R. Winston, J. Miñano, and P. Benítez, *Nonimaging Optics* (Elsevier, Boston, 2005), pp. 366–368.
[33] A. S. Brown, M. A. Green, and R. P. Corkish, Physica E (Amsterdam) **14**, 121 (2002).
[34] A. S. Brown and M. A. Green, Physica E (Amsterdam) **14**, 96 (2002).
[35] R. C. Alig, S. Bloom, and C. W. Struck, Phys. Rev. B **22**, 5565 (1980).
[36] Please note that the efficiencies that the authors present here are first-law efficiencies that are given as the photovoltaic power density generated by the converter divided by the total-energy flux impinging on the converter. Resulting from this, the efficiencies for nonconcentrated ($\times 1$) solar illumination that are reported elsewhere in the literature may be roughly 1.3 times larger than those that are reported here (cf. efficiencies reported in Refs. 21, 25, 29, and 34). As explained in Ref. 14, a second-law efficiency calculation that includes the energy flux from the Sun and that excludes the energy flux from the Earth will result in a distorted efficiency that is a factor $[1+(\frac{1-CD}{CD})(T_E/T_S)^4]$ larger than a calculation using the first-law efficiency that includes both. With respect to this factor, C and D are the geometric concentration and dilution factors, respectively, and T_E and T_S are the surface terrestrial and solar temperatures, respectively. The smaller the concentration factor is, the more pronounced is the distortion. For example, allowing that $D=2.16\times 10^{-5}$, $C=1$, $T_E=300$ K, and $T_S=6000$ K, then the distortion is given by a factor of $1+(4.63\times 10^4)(6.25\times 10^{-6})=1.29$.